# Distance-Dependent Proton Transfer along Water Wires Connecting Acid−Base Pairs

**M. Jocelyn Cox,[†] Rutger L. A. Timmer,[†] Huib J. Bakker,*[,†] Soohyung Park,[‡] and Noam Agmon*[,‡]**

*FOM-institute for Atomic and Molecular Physics, Kruislaan 407, 1098 SJ Amsterdam, The Netherlands, and Institute of Chemistry and the Fritz Haber Research Center, The Hebrew University of Jerusalem, Jerusalem 91904, Israel*

*Received: January 16, 2009; Revised Manuscript Received: April 20, 2009*

We report time-resolved mid-IR kinetics for the ultrafast acid−base reaction between photoexcited 8-hydroxypyrene-1,3,6-trisulfonic acid trisodium salt (HPTS), and acetate at three concentrations (0.5, 1.0, and 2.0 M) and three temperatures (5, 30, and 65 °C) in liquid $D_2O$. The observed proton-transfer kinetics agree quantitatively, over all times (200 fs−500 ps), with an extended Smoluchowski model which includes distance-dependent reactivity in the form of a Gaussian rate function, $k(r)$. This distance dependence contrasts with the exponential $k(r)$ that is typically observed for electron-transfer reactions. The width of $k(r)$ is essentially the only parameter varied in fitting the proton-transfer kinetics at each concentration and temperature. We find that $k(r)$ likely represents the rate of concerted (multi)proton hopping across "proton wires" of different length $r$ that connect acid−base pairs in solution. The concerted nature of the proton transfer is supported by the fact that $k(r)$ shows a steeper dependence on $r$ at higher temperatures.

## Introduction

Acid−base reactions are fundamental to chemistry and presented in almost every general chemistry textbook. In the conventional picture of solution-phase proton transfer (PT), an acid, AH, and a base, $B^-$, need to diffuse toward one another before the reaction can take place. Thus, Eigen and co-workers[1,2] have suggested a two-step mechanism in which an encounter complex, $AH\cdots B^-$, is formed by diffusion after which PT within this complex can occur

$$AH + B^- \underset{k_{-D}}{\overset{k_D}{\rightleftharpoons}} AH\cdots B^- \xrightarrow{k_0} A^- + HB \qquad (1)$$

Here, $k_D$ and $k_{-D}$ denote the diffusion-controlled encounter complex formation and dissociation rate coefficients, respectively, and $k_0$ is the intrinsic PT rate coefficient. The encounter complex (sometimes called the "contact pair") is thought to involve the acid and base molecules separated by one or two water molecules,[3] leading to a typical "contact distance", $a$, in the range of 6−7 Å.

In order to follow a PT reaction in the time domain, one needs to trigger the reaction at a well-specified time. The temperature jump methods developed by Eigen and co-workers allowed the study of PT reactions in the microsecond time regime, but faster PT reactions require an optical trigger. A specific class of molecules, called photoacids, change their p$K_a$ upon photoexcitation and as such are very suitable for this purpose. Early investigations into photoacids,[3] such as naphthols, have established the field of excited-state PT. When a photoacid, ROH, absorbs a photon, a cascade of events is initiated,[4] including intramolecular charge transfer, relaxation to the ground vibrational state of $S_1$, enhancement of the $ROH\cdots OH_2$ hydrogen bond, and reversible PT to solvent with the proton diffusing away from the $RO^-$ via the Grotthuss mechanism.[5] When a base is added to the solution, direct PT by the mechanism of eq 1 is expected to compete with PT to solvent.[6−9] To obtain a good estimate of $k_0$, independent of PT to the solvent and diffusion, the reaction was investigated at very high base concentrations (8 M).[10]

When the acid−base reaction is sufficiently downhill to be irreversible and the base is in large excess (pseudounimolecular conditions), the mechanism in eq 1 leads to Smoluchowski kinetics.[11−17] This description is valid for pseudounimolecular irreversible reactions, in which the initially randomly distributed base molecules react independently with the acid. The survival probability, $S(t)$, of the acid is then obtained as a product of the survival probabilities due to all base molecules.[13−15] The $AH/B^-$ pair kinetics are described by a diffusion equation. When the irreversible PT reaction occurs at a fixed distance, as implicitly assumed in eq 1, an appropriate boundary condition is imposed at this distance. Smoluchowski has utilized an absorbing boundary,[11] which can be generalized to a "radiation boundary condition" (with a rate parameter $k_0$),[18] as suggested by Collins and Kimball.[19] The resulting model, which is equivalent to having a delta function sink at the "contact distance" $r = a$, is referred to as the Smoluchowski−Collins−Kimball (SCK) model. When $k_0$ is sufficiently large, $S(t)$ decays initially with the rate coefficient $k_0$ and then slows down to an ultimate exponential decay characterized by a slower steady-state rate coefficient.

The SCK model was previously applied to fluorescence quenching.[20] For quenching driven by electron transfer (ET), difficulties with the SCK model were encountered, which could be overcome by replacing the delta function sink by a distance-dependent rate function, $k(r)$.[21−23] Such an approach was suggested theoretically by Wilemski and Fixman[24] and elaborated for photoinduced charge separation elsewhere.[25]

More recently, the SCK model was applied successfully to excited-state PT between 2-naphthol-6-sulfonate and acetate in glycerol−water solutions.[26,27] The high solvent viscosity slowed

* To whom correspondence should be addressed. E-mail: bakker@amolf.nl (H.J.B); agmon@fh.huji.ac.il (N.A.).
† FOM-institute for Atomic and Molecular Physics.
‡ The Hebrew University.

10.1021/jp9004778 CCC: $40.75 
Published on Web 05/18/2009

down the reaction to the regime conveniently probed by the time-correlated single-photon counting (TCSPC) technique. A similar analysis has been applied to the ground-state protonation of a photochemically generated $ONOO^-$ base.[28] For proton concentrations in the range of 100 mM, the SCK model gave good agreement with the measured kinetics.

A new era in the investigation of acid−base reactions began with the introduction of time-resolved IR spectroscopy as a probe of the transient PT kinetics.[29−36] Although this method has inferior signal/noise ratio as compared to TCSPC, it has much improved time resolution (essential for a highly reactive system), and it can follow the transient IR signal from both reactants and products. The system of choice here was the photoacid 8-hydroxy-1,3,6-pyrenetrisulfonic acid (HPTS), with acetate derivatives as the base. At high base concentrations, biphasic PT kinetics were observed,[29] where the fast phase (sub 150 fs) was attributed to PT within $ROH\cdots B^-$ pairs formed already in the ground state, and the slower phase was fit with the SCK model.[30] More recent work showed that the SCK model is inadequate even for the slow phase.[34−36] Chains of hydrogen-bonded water molecules ("proton wires") of different lengths supposedly connect the acid with the base, resulting in PT over distances bridged by several water molecules. The rate-limiting step in these reactions is the formation of a hydrogen-bonded configuration of the intervening water molecules that allows the transfer of the proton. Once an appropriate configuration for conduction is established, the transfer itself is ultrafast, in the femtosecond time regime. As a consequence, the product (acetic acid) IR signal rises instantaneously with the decay of the excited HPTS reactant.[29,34] This picture contrasts with suggestions that the proton can be temporarily trapped on an intervening water molecule[31,32,37] and agrees with quantum calculations showing PT along short proton wires occurring on the 100 fs time scale.[38−40] The motion of protons along short wires can be concerted and synchronous,[40,41] rather than stepwise. Likewise, it was shown that intramolecular PT through water molecule bridges mainly occurs via concerted double and triple PT.[42]

In ET reactions, the distance dependence of $k(r)$ depends on the free-energy difference between reactants and products. For highly exoergic ET reactions, $k(r)$ goes through a maximum at large distances due to the $r$ dependence of the reorganization energy in the Marcus−Hush theory.[43] For PT in water, the distance dependence is connected to the molecular structure of the medium (water). Interestingly, in bulk liquid water, no proton wires were identified. Rather, a sequence of hydrogen-bond reorganizations is suggested to drive proton hopping between adjacent water molecules.[44] Proton wires were detected (computationally) in pure liquid water only when water molecules were confined into a single file within a pore.[39] The formation of interconnecting proton wires for acid−base solutions can be stimulated by either the difference in acidity of the reacting partners or their ionic character.[45] The good agreement with the conventional SCK model previously observed for PT between 2-naphthol-6-sulfonate and acetate in glycerol−water mixtures[26,27] may be partly due to disruption of such wires by the glycerol cosolvent.

The present work investigates the temperature dependence of an exoergic excited-state PT between a photoacid (HPTS) and an anionic base (acetate),[29,34] which is suggested to occur via proton wires.[32−36] Assuming that PT through such wires is concerted,[40,41] the transfer across the whole wire can be described with a single distance-dependent rate constant, $k(r)$, in analogy to models of photoexcited electron transfer.[21,22] The ultrafast kinetic phase is expected to be sensitive to the functional form of $k(r)$, whereas the long-time phase will reflect the mutual acid−base diffusion.

## Theory Section

We aim to describe the time dependence of PT by a single distance-dependent rate coefficient $k(r)$. Extending the analogous treatment for ET reactions,[21,22] we consider a family of "sink terms" with the functional form

$$k(r) = k_0 \exp[-(r - a)^n/\sigma] \tag{2}$$

Here, $a$ is the distance of closest approach between acid and base ($r \geq a$), and $k_0$ is the maximal value of the rate coefficient attained at this distance. The power $n$ is a parameter which we hope to determine by comparison with the experiment, and $\sigma$ is a parameter that determines the width of $k(r)$. Practically, it will be the only adjustable parameter in our model.

In the theoretical treatment below, several approximations are invoked.

(1) The reaction is irreversible, which is valid if $pK_a(\text{base}) \gg pK_a(\text{acid})$.[46]

(2) The reaction is pseudounimolecular due to the high concentration, $c$, of the acetate base.

(3) The system is assumed to be spherically symmetric, even though the hydroxyl occupies a small fraction of the HPTS surface. For excited-state PT to solvent, such an approximation is routinely applied, and with good results.[4] However, the justification given there,[47] that the reaction is slow as compared with rotational diffusion, no longer holds in the present case. To our knowledge, an extension of the Smoluchowki theory to angular dependence has not been applied to experimental data; therefore, it is presently hard to assess its merits.

(4) There is no interaction potential between HPTS and acetate. Although both are negatively charged, neglect of their Coulombic repulsion is justified in the high concentration regime, where the electrostatic interaction is almost totally screened (by the sodium counterions).

In the first few picoseconds after photoexcitation, the molecules do not yet move. In this static limit, the survival probability of the protonated acid, $S(t)$, decays as

$$S(t) = \exp\{-c \int_a^\infty \mathrm{d}r 4\pi r^2 [1 - \mathrm{e}^{-k(r)t}]\} \tag{3}$$

Thus, in the $t \to 0$ limit, the decay is exponential

$$S(t) \sim \exp(-c\langle k\rangle t) \tag{4}$$

where the average rate constant is

$$\langle k\rangle \equiv \int_a^\infty \mathrm{d}r 4\pi r^2 k(r)$$

As time progresses, the acid−base partners start moving, with a mutual diffusion coefficient $D$, which is the sum of their individual diffusion coefficients. Assuming that $S(t)$ is the product of the acid survival probability due to the randomly distributed base molecules, and going to the continuum limit,[13−15] one obtains the survival probability of the generalized Smoluchowski form

$$S(t) = \exp[-cP(t)] \tag{5}$$

The pair reaction probability, $P(t)$, is calculated from its probability density, $p(r,t)$, by integrating the reactive flux

$$P(t) \equiv \int_0^t \mathrm{d}t' \int_a^\infty \mathrm{d}r 4\pi r^2 k(r) p(r, t') \tag{6}$$

Hence, eq 3 is a special case of eq 5 with $p(r,t) = \exp[-k(r)t]$, namely, a pair at separation $r$ reacts unimolecularly with a rate coefficient $k(r)$.

At longer times, diffusion starts to play a role, and $p(r,t)$ is obtained as the solution of a spherically symmetric diffusion equation with a sink term[24]

$$\frac{\partial p(r,t)}{\partial t} = \frac{D}{r^2}\frac{\partial}{\partial r}r^2\frac{\partial}{\partial r}p(r,t) - k(r)p(r,t) \qquad (7)$$

provided that initially $p(r,0) = 1$. Because the reaction is described by $k(r)$, one imposes a reflecting boundary condition at the contact distance, $a$, namely, $(\partial p(r,t)/\partial r)|_{r=a} = 0$. This equation is solved numerically, for example, by the SSDP application.[48]

The SCK model is the special case of the above, where

$$k(r) = k_0\delta(r - a)/(4\pi a^2) \qquad (8)$$

There are rather good analytical approximations to $S(t)$ for delta function (eq 8) or exponential sinks[16,17] but not for a more general distance dependence of $k(r)$. Because the short-time behavior in eq 3 depends only on $k(r)$ (and not on $D$), the data up to approximately 5 ps will be utilized to search for the optimal functional dependence in eq 2. With this $k(r)$ and the experimentally determined diffusion constants, eqs 5−7 are expected to fit the data over the whole time range.

## Experimental Section

We have studied the effects of temperature on the PT reactions between the photoacid 8-hydroxypyrene-1,3,6-trisulfonic acid trisodium salt (HPTS) and a base (acetate) in $D_2O$ using ultrafast visible pump−infrared probe spectroscopy. HPTS is a commonly used photoacid for these types of experiments because it has a strong absorption near 400 nm and can therefore be excited using the second harmonic of a Ti:Saphhire laser.

HPTS was promoted to an electronically excited state with a 100 fs laser pulse centered at 400 nm and probed using transient absorption of a broad-band infrared pulse. The infrared pulses were tuned to the transient resonances of the excited (*) photoacid seen in Figure 1: HPTS* (1480 $cm^{-1}$), the conjugate photobase, $PTS^{*-}$ (1503 $cm^{-1}$), the carbonyl vibration of the acetic acid band (1710 $cm^{-1}$), and the hydrated proton/deuteron (>1800 $cm^{-1}$). In the present work, we monitor the PT reactions primarily through the dynamics of the HPTS* band.

The 400 nm pump and the tunable infrared pulses are generated via nonlinear frequency conversion processes that are pumped by the pulses obtained from a regeneratively amplified Ti:Sapphire laser system (Spectra-Physics Hurricane). This system produces 100 fs, 1.1 mJ pulses centered at 800 nm with a repetition rate of 1 kHz. To generate the 400 nm pump pulse, a fraction (about 20%) of the 800 nm pulse was frequency doubled in a type-I BBO crystal (2 mm, $\theta = 29°$). To generate tunable infrared pulses, a BBO-based optical parametric amplification (OPA, SpectraPhysics) stage was used to convert the remaining fraction (about 80%) of the 800 nm pulse into two output pulses (1.2−2.5 $\mu$m). These pulses were focused into a $AgGaS_2$ crystal (2 mm, $\theta = 45°$). Difference frequency mixing of the two pulses in this crystal produced mid-infrared pulses that were tunable between 2.7 and 8 $\mu$m (3700−1250 $cm^{-1}$) with a pulse duration of ~150 fs and a frequency bandwidth of ~200 $cm^{-1}$.

The relative delay between the pump and mid-infrared pulses was set with a computer-controlled translation stage. The pump polarization was rotated with a polarizer to the magic angle (54.7°) relative to the probe pulses, so that only isotropic absorption changes were detected. A 50% beam splitter divided the mid-infrared pulse into probe and reference components. The probe and reference beams were focused into the sample by a parabolic mirror ($f = 150$ mm), and the 400 nm pump beam was focused by a lens with a focal length of 400 mm. Only the pump and probe beams overlap in the sample. The transmitted probe and reference pulses were dispersed with an Oriel spectrometer and detected by two lines of an Infrared Associates 2 × 32 MCT (mercury−cadmium−telluride) detector array.

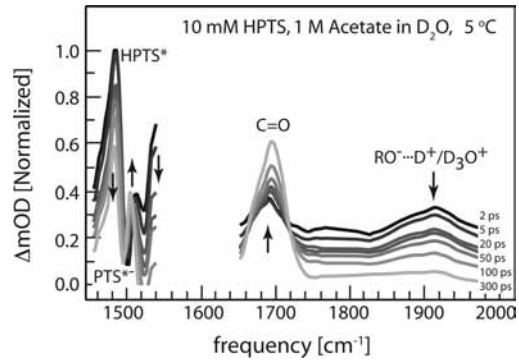


**Figure 1.** Transient mid-IR absorption spectra of 10 mM HPTS in liquid $D_2O$ solution containing 1 M sodium acetate at 5 °C and different delay times following the exciting 400 nm pulse.

In the experiment, we measured the change in mid-infrared absorption that results from the excitation by the pump beam. The frequency-resolved transmission of the sample is given by $I_p(\nu) = I_{p,in}(\nu)e^{-\alpha(\nu)}$, with $I_p(\nu)$ as the energy of the probe pulse transmitted through the sample, $I_{p,in}(\nu)$ as the input probe energy, and $\alpha(\nu)$ as the absorption. To determine the pump-induced change in absorption, the probe signals were alternatingly measured with and without a pump pulse present using a 500 Hz chopper in the pump beam. The absorption change $\Delta\alpha(\nu)$ is given by

$$\Delta\alpha(\nu) = \alpha(\nu) - \alpha_0(\nu) = -\ln\left[\frac{I_p(\nu)I_{p,in,0}(\nu)}{I_{p,in}(\nu)I_{p,0}(\nu)}\right] \qquad (9)$$

where the subscript 0 denotes the signals measured in the absence of the pump. The fraction $I_{p,in,0}(\nu)/I_{p,in}(\nu)$ in this expression can be replaced by $I_{r,0}(\nu)/I_r(\nu)$, where $I_{r,0}(\nu)$ and $I_r(\nu)$ represent the energies of the reference measured in the absence and presence of the pump beam, respectively. These signals are measured at the same time as $I_{p,0}(\nu)$ and $I_p(\nu)$. Thereby, the reference serves to normalize the measured signal with respect to the pulse to pulse fluctuations in the probe pulse energy. We thus arrive at

$$\Delta\alpha(\nu) = -\ln\left[\frac{I_p(\nu)I_{r,0}(\nu)}{I_r(\nu)I_{p,0}(\nu)}\right] \qquad (10)$$

The $\Delta\alpha(\nu)$ represents the frequency-dependent change in absorption in the mid-infrared due to the excitation of HPTS molecules by the 400 nm pump. This absorption change is comprised of both increases in absorption signals, arising from the excited HPTS* molecules and/or their reaction products, and decreases in absorption signals due to the depletion of HPTS in the ground state.

The signals were averaged over 5000 shots at each delay time. The sample was contained in a rotating temperature-controlled cell between two $CaF_2$ windows separated by a 50−100 $\mu$m spacer. The sample was rotated to avoid photoproduct formation and long-term heating effects. Attenuation of the pump pulse to 1 $\mu$J per pulse prevented any multiphoton effects. The samples each contained 10 mM HPTS (8-hydroxy-1,3,6-pyrenetrisulfonic acid trisodium salt, Aldrich 98%) dissolved in $D_2O$ (Aldrich,

99.9%). The concentration, $c$, of the acetate base ($CH_3COONa$, Aldrich 99%) was varied (0.5, 1, and 2 M), and the reaction was measured at different temperatures (5, 30, and 65 °C).

## Results

Figure 1 shows the transient absorption spectra measured for a solution of 10 mM HPTS and 1 M acetate in $D_2O$. The spectra show the transient response in the infrared region of the aromatic ring vibrations of HPTS* and PTS*$^-$, the carbonyl stretching vibration, and the deuteron continuum.[36] After electronic excitation of HPTS to its excited singlet state, there is a direct rise of the IR absorption at 1480 and 1540 $cm^{-1}$, which we assign to HPTS*. At longer delay times, these absorptions decay, and a new absorption at 1503 $cm^{-1}$ grows in, which is assigned to the conjugate photobase, PTS*$^-$. Figure 1 also shows the transient spectrum between 1650 and 2000 $cm^{-1}$, containing the carbonyl stretching of the acetic acid centered at 1710 $cm^{-1}$ and the broad-band infrared absorption that we attribute to the deuteron signal.[36] The rise of the carbonyl absorption (coinciding with the decay of the deuteron absorption) signals the arrival of the deuteron at the acetate base to form acetic acid. In the following, we will focus primarily on the dynamics of the HPTS* band.

The data sets consist of a matrix of pump-induced, frequency ($\nu$), and time-resolved absorption difference measurements $\Delta\alpha(t,\nu)$ and their corresponding standard deviations $\varepsilon(t,\nu)$. These absorption differences are assumed to arise as a result of two spectral responses, $\zeta(\nu)$, that are proportional to the time-dependent populations in either the HPTS* or PTS*$^-$ state

$$\Delta\alpha(t,\nu) = N_{HPTS}(t)\zeta_{HPTS}(\nu) + N_{PTS^-}(t)\zeta_{PTS^-}(\nu) \tag{11}$$

Furthermore, it is assumed that the total population of excited HPTS* + PTS*$^-$ is conserved, that is, $N_{HPTS} + N_{PTS^-} = 1$. This assumption is valid because the excited-state decay is negligible on the time scale of the measurements. The spectral responses of HPTS* and PTS*$^-$ are estimated by taking the spectra for $\Delta\alpha$ at early and late pump−probe delay times, respectively. Next, the population occupying the HPTS* state is calculated for all times $t$ by minimization of

$$\chi^2(\tilde{N}) = \int d\nu \left( \frac{\Delta\alpha(t,\nu) - \tilde{N}\zeta_{HPTS}(\nu) - (1-\tilde{N})\zeta_{PTS^-}(\nu)}{\varepsilon(t,\nu)} \right)^2 \tag{12}$$

The least-squares fitting value for $\tilde{N}(t)$ is calculated by equating the derivative of the above expression to 0. The value of $\tilde{N}(t)$ thus obtained is proportional to the population $N_{HPTS}$ at time $t$. This results in a model-independent estimate for the amount of population residing in either state at each time.

On the subpicsecond time scale, there is an intense coherent peak that interferes with the population dynamics. Due to this peak, $N_{HPTS}$ determined from the above procedure is not properly normalized. We can overcome this problem by monitoring the signal of the carbonyl stretching vibration of the acetic acid product at 1710 $cm^{-1}$ because this band provides a direct measure of completed proton-transfer events (Figure 2). Rini et al.[29] observed the fractions of acetic acid formed within their 150 fs resolution to be 0.11, 0.24, and 0.39 at 0.5, 1, and 2 M acetate, respectively. We find similar numbers from the analysis of the carbonyl band shown in Figure 2. This figure shows an initial contribution within the time resolution of ~200 fs with an amplitude that agrees well with the results of Rini et al.[29] We therefore normalize $N_{HPTS}$ at 1 ps (where the coherent process is mostly over) to 0.89, 0.76, and 0.61 at 0.5, 1, and 2 M acetate, respectively.

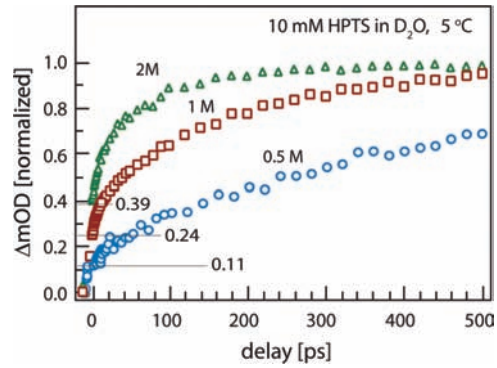


**Figure 2.** Time-resolved IR signal of the carbonyl vibration of acetic acid measured at 1710 $cm^{-1}$ for three different acetate concentrations. The signals contain an initial contribution (not shown) that results from ultrafast (<150 fs) proton transfer in directly hydrogen-bonded HPTS−acetate reaction complexes. The amplitudes at 1 ps are marked in the figure.

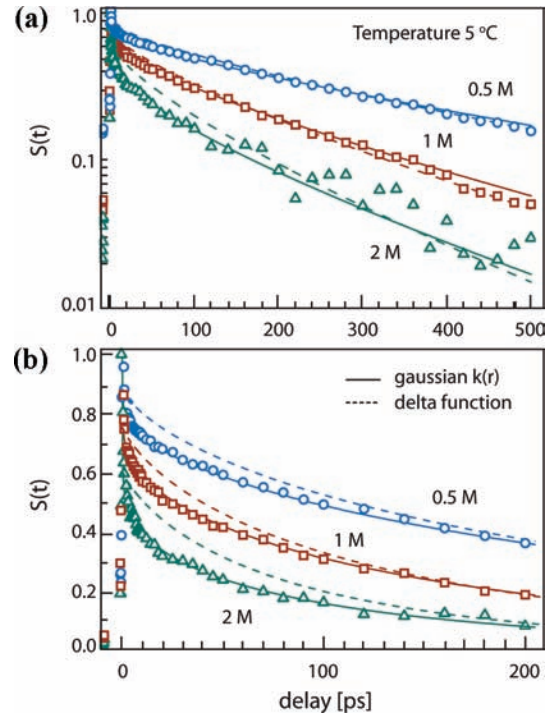


**Figure 3.** Time-resolved IR signals (symbols) from excited HPTS in $D_2O$ at 5 °C and three acetate concentrations, normalized at 1 ps (to 0.89, 0.76, and 0.61 for $c$ = 0.5, 1, and 2 M acetate, respectively) are depicted as symbols on two different time scales, (a) semilogarithmic (up to 500 ps) and (b) linear (up to 200 ps). Dashed/full lines are fits to the solution of eqs 5−7 with two different sink terms, (i) delta function sink (dashed lines), eq 8, with $a$ = 6.8 Å and $k_0$ = 100, 60, and 35 $ns^{-1}$ for $c$ = 0.5, 1, and 2 M acetate, respectively, and (ii) Gaussian sink term, eq 2, with $n$ = 2 and parameters in Tables 1 and 2 (full lines).

The normalized time-resolved IR signal from HPTS* (1480 $cm^{-1}$) in $D_2O$ and three acetate concentrations at 5 °C are shown in Figure 3. The signal drops significantly on the subpicsecond time scale, indicating an initially very fast acid−base reaction.[29] After the first picosecond, the decay of the signal becomes more moderate.

The theoretical lines in Figure 3 were obtained from a numerical solution of eq 7 using the publicly available Windows application for solving the spherically symmetric diffusion

**TABLE 1: Estimated Relative Diffusion Coefficients (in $10^{-6}$ cm$^2$/s) between HPTS and Acetate, $D \equiv D_{HPTS} + D_{Ac^-}$, in Liquid $D_2O$ Containing NaAc Salt at Different Concentrations (rows) and Different Temperatures (columns) (see *Supporting Information* for further detail)**

| $c$, M | 5 °C | 30 °C | 65 °C |
|---|---|---|---|
| 0.5 | 6.9 | 14.0 | 26.7 (26.0)[a] |
| 1.0 | 5.9 | 12.1 (11.5) | 23.1 |
| 2.0 | 4.5 (3.5) | 9.1 (7.0) | 17.4 (17.0) |

[a] Values in parentheses are those actually used in the fits (when different from the estimated ones).

**TABLE 2: Fitting Parameter $\sigma$ (in Å$^2$) for $k(r)$ of Equation 2 with $n = 2$, $k_0 = 10^{14}$ s$^{-1}$, $a = 2.8$ Å, and $D$ from Table 1**

| $c$, M | 5 °C | 30 °C | 65 °C |
|---|---|---|---|
| 0.5 | 1.5 | 1.2 | 0.7 |
| 1.0 | 1.2 | 1.0 | 0.9 |
| 2.0 | 1.1 | 0.9 | 0.8 |

problem (SSDP, version 2.66).[48] This program also performs the integral in eq 6 and can be used to compare graphically $S(t)$ from eq 5 with the experimental data for $N_{HPTS}$. With the SCK model (delta function sink term, eq 8), it was not possible to get a good description of the very early time dynamics (<1 ps), and thus, in Figure 3, we only give the best fits (dashed lines) with the SCK model for $t > 1$ ps (renormalizing the calculation at 1 ps as described above). In these fits, we have set the "contact radius" (distance of minimal approach), $a$, to 6.8 Å (the precise value has little effect on the quality of the fit), corresponding to an acid−base separation of at least one water molecule.[3] It is seen that the SCK model is inappropriate for $t < 100$ ps, which we remedy by determining a more suitable functional form for $k(r)$.

Considering next the family of functions $k(r)$ defined in eq 2, we search for an optimal value for $n$ for which the theoretical $S(t)$ fits the experimental data over the entire time scale. Given that the early dynamics are due to directly hydrogen-bonded pairs,[29] this means that $k(r)$ depicts the PT reaction over all distances from the hydrogen-bond distance of 2.8 Å outward. Hence, we set $a \approx 2.8$ Å in eq 2. The optimal value of $n$ was subsequently determined from the short-time kinetics as follows.

For each concentration and each value of $n = 1$, 2, and 3, we have first fitted the entire time dependence of $N_{HPTS}$ to $S(t)$ from eqs 5−7. These solutions were subsequently convoluted with a Gaussian instrument response function of 500 fs full-width at half-maximum (fwhm) and shifted from the time origin by 250 fs. Figure 4 shows this comparison using the data from Figure 3 on an expanded scale, focusing on the first few picoseconds. Due to the presence of the coherence peak at $t <$ 1 ps, the differences between the fits for different $n$ are observed best at the highest concentration (2 M). It is seen that a fit with $n = 1$ (exponential sink) is somewhat inferior to fits with $n =$ 2 or 3 (the latter two giving similar results). Therefore for the remainder of this work, we have selected a Gaussian sink, $n = 2$.

In addition to globally fixing $a$ and $n$, the on-contact rate constant in eq 2 was given a large and constant value, $k_0 = 10^{14}$ s$^{-1}$. This leaves only two parameters to be adjusted at each value of $c$ and $T$, namely, $\sigma$ and $D$. Unfortunately, there are no directly measured values of $D$ available. Variation of $D$ does not affect the ultrafast phase but does affect rather strongly

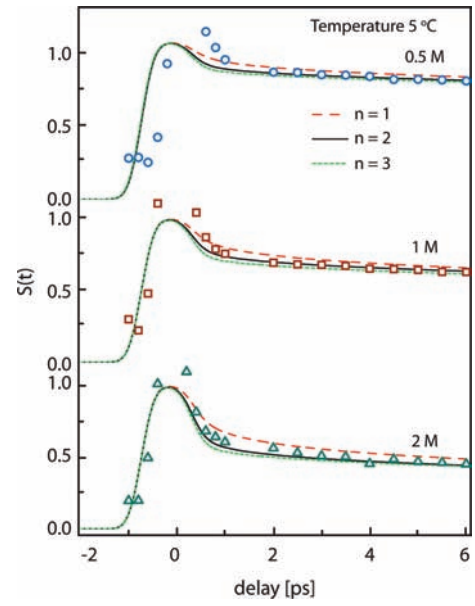


**Figure 4.** The data from Figure 3, on a linear scale and up to 6 ps, is compared with the theoretical solution, which is convoluted with an IRF of 500 fs fwhm. The values of $D$ used in the calculation are given in Table 1. For $n = 2$ (full lines), the values of $\sigma$ are collected in Table 2 (see eq 2). The best fits for $n = 1$ and 3 are shown by the dashed lines. The values of $\sigma$ for $n = 1$ are 0.44, 0.4, and 0.37 Å for $c = 0.5$, 1, and 2 M, respectively, while for $n = 3$, they are 5.0, 3.7, and 3.0 Å$^3$.

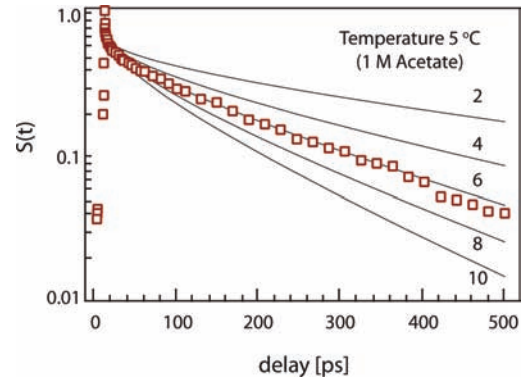


**Figure 5.** The effect of varying the diffusion constant on the acid−base kinetics, demonstrated for the reaction of HPTS* with 1.0 M acetate at 5 °C (same data as that in Figure 3). The lines were calculated with $\sigma = 1.2$ Å$^2$ (see Table 2) and the indicated values of $D$ (in units of $10^{-6}$ cm$^2$/s).

the longer time kinetics, as demonstrated in Figure 5. With increasing values of $D$, the HPTS−acetate collision events become more frequent, leading to faster PT kinetics.

In order to limit the variation of $D$ in the fitting procedure, we have adopted the following approach. We have assumed that in water, $D = 1.0 \times 10^{-5}$ cm$^2$/s at 25 °C and 2 M acetate, and we obtained $D(T,c)$ in $D_2O$ by utilizing experimental data for $D_2O$ viscosities as a function of temperature[49] and concentration.[50] The underlying assumption here is the validity of the Stokes−Einstein relation between the diffusion constant and viscosity. The analysis is detailed in the Supporting Information, with the ensuing values of $D$ summarized in Table 1. In the final fits, a few values of $D$ are somewhat different from those in Table 1. These values are shown in parentheses there.

Using predetermined values of $D$ leaves only a single adjustable parameter, $\sigma$, in fitting the kinetics at the nine combinations of $c$ and $T$; see Table 2. Figure 3 shows the fits

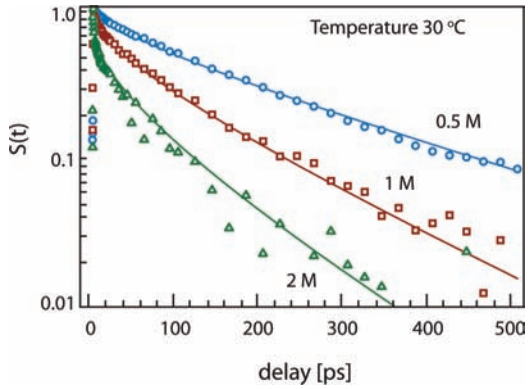


**Figure 6.** Near-IR kinetics for PT between HPTS* and acetate at 30 °C. Other details as in Figure 3.

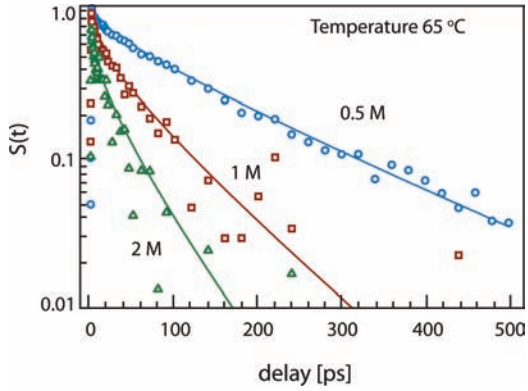


**Figure 7.** Near-IR kinetics for PT between HPTS* and acetate at 65 °C. Other details as those in Figure 3.

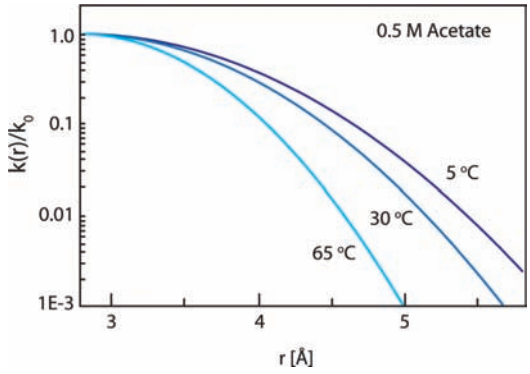


**Figure 8.** Temperature dependence of the distance-dependent rate constant for PT between HPTS* and 0.5 M acetate, using the values of $\sigma$ from Table 2.

to the 5 °C data as solid lines, whereas Figures 6 and 7 show these fits at the two higher temperatures, 30 and 65 °C, respectively. Although the noise in the experimental data increases with increasing $T$, it is apparent that the model provides a good description of the experimental results at all temperatures. The values of $\sigma$ (Table 2) obtained from these fits decrease with increasing $T$, meaning that $k(r)$ decays more rapidly with $r$ at higher temperatures. At the lowest concentration of 0.5 M, $\sigma$ shows the strongest decrease with temperature. The dependence of $k(r)$ on $T$ in this case is depicted in Figure 8.

The reactive flux density in our model is given by $k(r)p(r,t)$. The reactive flux density multiplied by $r^2$ depicts the radial reaction flux density at different acid−base separations. Figure 9 shows this function at different times for the lowest temperature and concentration measured in this study. Because at $t = 0$ we have $p(r,0) = 1$, the flux density is initially equal to $k(r)$

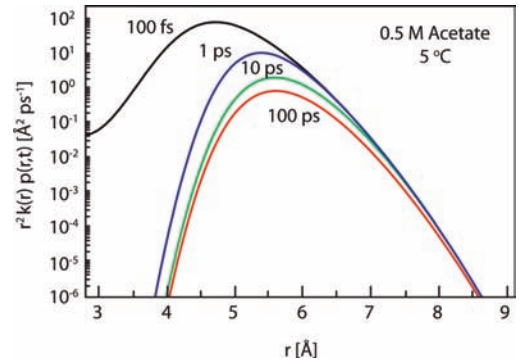


**Figure 9.** The distance dependence of the radial reactive flux density for PT between HPTS* and 0.5 M acetate at 5 °C, with $\sigma = 1.5$ Å$^2$ (Table 2).

and thus peaks at $r = a$. At $t = 100$ fs, most of the reaction still takes place close to contact, within directly bound acid−base pairs. By $t = 1$ ps, we get a flux peaking at around 5 Å, which corresponds to acid and base separated by one water molecule. This distribution has a tail to large distances. Because the peak diminishes strongly with time, the relative contribution of this tail increases with $t$, and it corresponds to proton wires containing more than one water molecule.[34] The long-$r$ tails show the onset of diffusive motion as follows. At short times, when the population is static, $k(r)p(r,t)r^2$ tends to the same large $r$ asymptotes. A similar inhomogeneous limit was previously recognized in the short-time behavior of carbon monoxide binding to myoglobin.[51] As diffusion sets in, the outer part of the distribution moves inward to compensate for reacting pairs, as seen in the long-$r$ tail for $t = 100$ ps.

## Discussion

According to the traditional view of PT in solution,[1,2] acid and base molecules diffuse first to a "contact distance" at which they are separated by one water molecule ("inner-sphere" mechanism). At this particular distance, the PT reaction takes place. However, from the present and previous femtosecond mid-infrared experiments, it follows that there exists a range of distances at which the proton can be transferred from the acid to the base.[32−36]

At very early times (<1 ps), a very rapid simultaneous decay of the HPTS* band and rise of the acetic acid carbonyl band are observed. This phase reflects an ultrafast PT reaction most likely occurring in acid−base pairs that were directly hydrogen-bonded already in the ground state.[29,30] At longer times, the observed decay becomes much slower and considerably more sensitive to temperature. The dynamics of this slower phase was originally attributed to diffusion, bringing the acid−base pair into contact. Following a successful application of the SCK model to acid−base reactions in glycerol−water mixtures,[26,27] Rini et al.[29,30] have applied this model to the HPTS/acetate system. However, the experimental data deviates from exponential behavior more than that predicted by the SCK model, as illustrated in Figure 3. To explain these observations, Rini et al.[29,30] and later Mohammed et al.[31−33] introduced additional subsets of acid−base complexes with different kinetics to fit the data. The final model involved coupled kinetic equations for sequential proton hopping along water chains of different lengths, with additional rate constants for changing the chain length, totalling in some two dozen adjustable parameters (including the ultimate diffusion process).[33] Siwick et al. also found evidence for PT taking place in a distribution of hydrogen-bound reaction complexes that differ in the number of water

molecules separating the acid and the base.[34,35] The observed PT kinetics could be modeled well by assuming that the distribution of reaction complexes is statistical (only determined by the base concentration) and that the rate of PT within a complex scales down by a constant factor for every additional water molecule in the chain separating the acid and the base. This description implies that the rate constant of PT is assumed to depend exponentially on the length of the water wire connecting the acid and the base.

Here, we have fit the whole time dependence of the PT kinetics (including the femtosecond phase) with a single distance-dependent rate coefficient, $k(r)$, adjusting essentially a single parameter $\sigma$ at each $c$ and $T$. We found from the short-time kinetics that PT is best described by a Gaussian-shaped $k(r)$ (see Figure 4). Our model is mathematically similar to the Wilemski−Fixman[24] model applied to fluorescence quenching by electron transfer in solution.[21−23] Because a Gaussian starts to decay rapidly only beyond a certain distance $r$, its $r$ dependence is qualitatively similar to assuming static quenching within an inner spherical shell and exponential quenching outside of it.[22] Despite these formal similarities between the ET studies and the present study of PT, the physical mechanisms responsible for the distance dependencies are different. For ET reactions, the distance dependence is thought to reflect the exponential decay of the electronic wave function at large distances. Hence, for ET, the coupling is through space. For PT, the reaction is not through space but proceeds through more or less randomly coiled water wires, and this could lead to a Gaussian dependence of the transfer rate on the radial distance $r$ as follows.

Suppose the water wire forms a freely joint chain (no angular restrictions). The mean end-to-end distance, $\langle (r - a)^2 \rangle^{1/2}$, of the water wire is then proportional to the square root of $N$, the number of water molecule monomers, by[52] $\langle (r - a)^2 \rangle^{1/2} = N^{1/2}L$, where $L$ is the distance between the water molecules (∼2.8 Å). From this relation, it follows that the Gaussian-shaped $k(r)$ corresponds to an exponential dependence on the water wire length $NL$, $k(N) = k_0 \exp(-NL/\sigma')$, with $\sigma' = \sigma/L$. This argument may explain a Gaussian $k(r)$ for long chains. However, it should be realized that the angles between the hydrogen bonds in the water wire are not arbitrary, and the water wires will contain only a limited number of water molecules. For short wires, it is thus possible that the functional form of $k(r)$ arises from a different origin such as quantum effects. This relation therefore requires further study.

A central question is how PT across these "proton wires" takes place. Previous work argued for a sequential single PT mechanism, in which the proton released from the photoacid hops along the wire until it eventually reaches the base.[29−33] This scenario supports a localized $D_3O^+$ cation on a water molecule separating the acid and base,[31] based on the observation of a broad-band absorption at around 1900 $cm^{-1}$ (cf. Figure 1). This band was more recently attributed to a weakened RO−H bond of HPTS* following excitation.[34,35] In a sequential scenario, if each hop between a pair of water molecules took 1−2 ps as that in liquid water,[53] crossing the chain would induce a picosecond delay between the rise in the acetic acid signal and the decay of the HPTS absorption, which is not observed. In addition, we find here that PT can be described by a single rate constant, $k(r)$, rather than a series of rate constants for sequential proton hops as previously assumed.[33]

An alternative scenario that is consistent with our findings is a concerted mechanism. Concerted proton transfer means that in chains of $N$ water molecules connecting acid and base, $N + 1$ protons move simultaneously and unidirectionally, each hopping across a single hydrogen bond. The concerted scenario is not only supported by the absence of any delay between the photoacid decay and the rise of acetic acid signal but also by the measured temperature effect. In a sequential scenario, each hopping event should become more rapid with increasing temperature, as is the case for proton mobility in liquid water.[5] Therefore, if $k(r)$ were an "effective" function depicting the overall transfer rate, it should have increased with increasing temperature. In the present case, the opposite is observed. The parameter $\sigma$ in eq 2 decreases with increasing $T$ (see Table 2), implying that $k(r)$ decreases with increasing $T$ for $r > a$, as seen Figure 8. This decrease can be explained by the enhanced disorder that disrupts the wire structure that is required for the concerted proton-transfer process to occur.

Concerted double and triple PT is a common observation in intramolecular PT through water molecule bridges.[42] Intermolecularly, synchronous multiproton motion was observed in quantal simulations of PT along a proton wire in carbonic anhydrase[41] and the green fluorescent protein (GFP).[40] For GFP, the proton released from the photoexcited chromophore hops to a nearby water molecule at the same time as another proton hops from this water to Ser205 and a third proton moves from Ser205 to Glu222. Related to these observations, it was found that the proton dissociation rate coefficient for GFP increases as $T$ is decreased from room temperature to 230 K (Figure 6 in ref 54). Although the time resolution of the TCSPC system utilized there is inferior to that of the present method (and the quantal calculations), such an inverse temperature dependence may nevertheless reflect an increasing probability for concerted multiproton transfer to occur at lower temperatures.

The conditions for concerted transfer are thus clearly different from those promoting incoherent PT between water molecules in the liquid phase.[5] In liquid water, PT along extended hydrogen-bonded chains of water molecules was observed (computationally) only within a narrow pore that restricts the water configuration to a single file traversing the pore. The proton mobility along such chains can be over 10 times faster than that of bulk liquid water.[39] In the chain, the coordination number of the water molecules is reduced, each water molecule being engaged in only two hydrogen bonds. In particular, one of the "donor" hydrogen bonds which normally stabilizes the hydronium structure is missing. This hydrogen bond strength is estimated to be markedly larger (∼20 kJ/mol) as compared to the average hydrogen bond of bulk water (∼11 kJ/mol).[55] Because a hydronium structure cannot be stabilized on any water molecule along the pathway, the concerted scenario becomes dominant.

## Conclusions

We studied the mechanism of proton transfer between the photoacid 8-hydroxypyrene-1,3,6-trisulfonate (HPTS) and the base acetate with femtosecond mid-infrared spectroscopy. In this study, we varied both the base concentration (0.5, 1, and 2 M) and the temperature (5, 30, and 65 °C). We find that the data cannot be fitted with the conventional Smoluchowski−Collins−Kimball (SCK) model in which the proton transfer is assumed to occur only at a particular acid−base separation. Instead, we find that the data at all studied concentrations, temperatures, and times can be best described with a distance-dependent rate function $k(r)$ that shows a Gaussian dependence on $r$. The distance $r$ is related to the length of the hydrogen-bonded water wires connecting the acid and the base. If the conformation of the water wires can be approximated as freely

joint chains, $r$ shows a square root dependence on the length of the water wires, which implies that the Gaussian dependence of $k(r)$ on the radial coordinate $r$ corresponds to an exponential dependence on the length of the water wires.

We find several indications that the proton transfer is a concerted process in which the proton is conducted from the photoacid to the base via hydrogen-bonded chains of intervening water molecules. The concerted nature of the proton transfer is supported by the observation that the signal associated with the proton arriving at the base rises simultaneously with the decay of the photoacid signal. In addition, we find that the parameter $\sigma$ and hence also $k(r)$ at $r > a$, eq 2, decrease with increasing temperature. Had the proton transfer proceeded via a sequential hopping process, the PT rate would have increased with temperature. The inverse temperature dependence of the concerted process can be explained from the fact that the increased disorder of the water solvent disrupts the water chain structures that are required for the concerted proton transfer to occur.

**Acknowledgment.** The research presented in this paper is part of the research program of the Stichting Fundamenteel Onderzoek der Materie (Foundation for Fundamental Research on Matter) and was made possible by financial support from the Nederlandse Organisatie voor Wetenschappelijk Onderzoek (Netherlands Organization for the Advancement of Research) (HJB). The research is also supported by the Israel Science Foundation (Grant Number 122/08) (NA). The Fritz Haber Center is supported by the Minerva Gesellschaft für die Forschung, München, FRG.

**Note Added after ASAP Publication.** This article posted ASAP on May 12, 2009. Due to a production error the paragraph after equation 9 has been revised. The correct version posted May 21, 2009.

**Supporting Information Available:** Estimation of diffusion coefficients from viscosity data. This material is available free of charge via the Internet at http://pubs.acs.org.

## References and Notes

(1) Eigen, M.; De Maeyer, L. *Proc. R. Soc. London, Ser. A* **1958**, *247*, 505–533.
(2) Eigen, M.; Kruse, W.; Maass, G.; De Maeyer, L. *Prog. React. Kinet.* **1964**, *2*, 287–318.
(3) Weller, A. *Prog. React. Kinet.* **1961**, *1*, 187–214.
(4) Agmon, N. *J. Phys. Chem. A* **2005**, *109*, 13–35.
(5) Agmon, N. *Chem. Phys. Lett.* **1995**, *244*, 456–462.
(6) Weller, A. *Z. Elektrochem.* **1954**, *58*, 849–853.
(7) Weller, A. *Z. Phys. Chem. N.F.* **1958**, *17*, 224–245.
(8) Trieff, N. M.; Sundheim, B. R. *J. Phys. Chem.* **1965**, *69*, 2044–2059.
(9) Laws, W. R.; Brand, L. *J. Phys. Chem.* **1979**, *83*, 795–802.
(10) Pines, E.; Magnes, B.-Z.; Lang, M. J.; Fleming, G. R. *Chem. Phys. Lett.* **1997**, *281*, 413–420.
(11) von Smoluchowski, M. *Z. Phys. Chem.* **1917**, *92*, 129–168.
(12) Pedersen, J. B.; Sibani, P. *J. Chem. Phys.* **1981**, *75*, 5368–5372.
(13) Tachiya, M. *Radiat. Phys. Chem.* **1983**, *21*, 167–175.
(14) Szabo, A.; Zwanzig, R.; Agmon, N. *Phys. Rev. Lett.* **1988**, *61*, 2496–2499.
(15) Szabo, A. *J. Phys. Chem.* **1989**, *93*, 6929–6939.
(16) Zhou, H.-X.; Szabo, A. *Biophys. J.* **1996**, *71*, 2440–2457.
(17) Dudko, O. K.; Szabo, A. *J. Phys. Chem. B* **2005**, *109*, 5891–5894.
(18) Carslaw, H. S.; Jaeger, J. C. *Conduction of Heat in Solids*, 2nd ed.; Oxford University Press: Oxford, U.K., 1959.
(19) Collins, F. C.; Kimball, G. E. *J. Colloid Sci.* **1949**, *4*, 425–437.
(20) Sikorski, M.; Krystkowiak, E.; Steer, R. P. *J. Photochem. Photobiol. A: Chem.* **1998**, *117*, 1–16.
(21) Song, L.; Dorfman, R. C.; Swallen, S. F.; Fayer, M. D. *J. Phys. Chem.* **1991**, *95*, 3454–3457.
(22) Shannon, C. F.; Eads, D. D. *J. Chem. Phys.* **1995**, *103*, 5208–5223.
(23) Murata, S.; Matsuzaki, S. Y.; Tachiya, M. *J. Phys. Chem.* **1995**, *99*, 5354–5358.
(24) Wilemski, G.; Fixman, M. *J. Chem. Phys.* **1973**, *58*, 4009–4019.
(25) Burshtein, A. I. *Adv. Chem. Phys.* **2000**, *114*, 419–587.
(26) Cohen, B.; Huppert, D.; Agmon, N. *J. Am. Chem. Soc.* **2000**, *122*, 9838–9839.
(27) Cohen, B.; Huppert, D.; Agmon, N. *J. Phys. Chem. A* **2001**, *105*, 7165–7173.
(28) Keiding, S. R.; Madsen, D.; Larsen, J.; Jensen, S. K.; Thøgersen, J. *Chem. Phys. Lett.* **2004**, *390*, 94–97.
(29) Rini, M.; Magnes, B.-Z.; Pines, E.; Nibbering, E. T. J. *Science* **2003**, *301*, 349–352.
(30) Rini, M.; Pines, D.; Magnes, B.-Z.; Pines, E.; Nibbering, E. T. J. *J. Chem. Phys.* **2004**, *121*, 9593–9610.
(31) Mohammed, O. F.; Pines, D.; Dreyer, J.; Pines, E.; Nibbering, E. T. J. *Science* **2005**, *310*, 83–86.
(32) Mohammed, O. F.; Pines, D.; Nibbering, E. T. J.; Pines, E. *Angew. Chem., Int. Ed.* **2007**, *46*, 1458–1461.
(33) Mohammed, O. F.; Pines, D.; Pines, E.; Nibbering, E. T. J. *Chem. Phys.* **2007**, *341*, 240–257.
(34) Siwick, B. J.; Bakker, H. J. *J. Am. Chem. Soc.* **2007**, *129*, 13412–13420.
(35) Siwick, B. J.; Cox, M. J.; Bakker, H. J. *J. Phys. Chem. B* **2008**, *112*, 378–389.
(36) Cox, M. J.; Bakker, H. J. *J. Chem. Phys.* **2008**, *128*, 174501.
(37) Leiderman, P.; Genosar, L.; Huppert, D. *J. Phys. Chem. A* **2005**, *109*, 5965–5977.
(38) Decornez, H.; Hammes-Schiffer, S. *Isr. J. Chem.* **1999**, *39*, 397–407.
(39) Brewer, M. L.; Schmitt, U. W.; Voth, G. A. *Biophys. J.* **2001**, *80*, 1691–1702.
(40) Vendrell, O.; Gelabert, R.; Moreno, M.; Lluch, J. M. *J. Phys. Chem. B* **2008**, *112*, 5500–5511.
(41) Cui, Q.; Karplus, M. *J. Phys. Chem. B* **2003**, *107*, 1071–1078.
(42) Kyrychenko, A.; Waluk, J. *J. Phys. Chem. A* **2006**, *110*, 11958–11967.
(43) Brunschwig, B. S.; Ehrenson, S.; Sutin, N. *J. Am. Chem. Soc.* **1984**, *106*, 6858–6859.
(44) Markovitch, O.; Chen, H.; Izvekov, S.; Paesani, F.; Voth, G. A.; Agmon, N. *J. Phys. Chem. B* **2008**, *112*, 9456–9466.
(45) Agmon, N. *J. Phys. Chem. A* **1998**, *102*, 192–199.
(46) Agmon, N. *Int. J. Chem. Kinet.* **1981**, *13*, 333–365.
(47) Pines, E.; Huppert, D.; Agmon, N. *J. Chem. Phys.* **1988**, *88*, 5620–5630.
(48) Krissinel′, E. B.; Agmon, N. *J. Comput. Chem.* **1996**, *17*, 1085–1098.
(49) Cho, C. H.; Urquidi, J.; Singh, S.; Robinson, G. W. *J. Phys. Chem. B* **1999**, *103*, 1991–1994.
(50) Genosar, L.; Cohen, B.; Huppert, D. *J. Phys. Chem. A* **2000**, *104*, 6689–6698.
(51) Agmon, N. *Biochemistry* **1988**, *27*, 3507–3511.
(52) Flory, P. J. *Statistical Mechanics of Chain Molecules*; Interscience: New York, 1969.
(53) Meiboom, S. *J. Chem. Phys.* **1961**, *34*, 375–388.
(54) Leiderman, P.; Huppert, D.; Agmon, N. *Biophys. J.* **2006**, *90*, 1009–1018.
(55) Markovitch, O.; Agmon, N. *J. Phys. Chem. A* **2007**, *111*, 2253–2256.

JP9004778